Hindawi
Mathematical Problems in Engineering
Volume 2019, Article ID 6278365, 10 pages
https://doi.org/10.1155/2019/6278365

Research Article

Design, Construction, and Operation of a High-Energy Mill for Handling Magnesium Powder

J. C. Paredes Rojas,[1] **L. E. Álvarez Ramírez**,[2] **G. Urriolagoitia Sosa**,[2] **C. R. Torres San Miguel**,[2] **B. Romero Ángeles**,[2] **J. A. Leal Naranjo**,[3] **and G. M. Urriolagoitia Calderón**[2]

[1] *Instituto Politécnico Nacional, Laboratorio Nacional de Desarrollo y Aseguramiento de la Calidad en Biocombustibles (LANDACBIO), Centro Mexicano para la Producción más Limpia, Acueducto de Guadalupe s/n, La Laguna Tecomán, 07340, Ciudad de México, Mexico*
[2] *Instituto Politécnico Nacional, Sección de Estudios de Posgrado e Investigación de la Escuela Superior de Ingeniería Mecánica y Eléctrica, Unidad Profesional "Adolfo López Mateos" de México, Edificio 5 Tercer Piso, Del. Gustavo A. Madero, Col. Lindavista, 07738, Mexico*
[3] *Departamento de Electrónica, DICIS, Universidad de Guanajuato, Carr. Salamanca-Valle de Santiago Km 3.5+1.8, Comunidad de Palo Blanco, 36885 Salamanca, GTO, Mexico*

Correspondence should be addressed to J. C. Paredes Rojas; paredesrojasjc@gmail.com

Received 30 October 2018; Revised 23 December 2018; Accepted 22 January 2019; Published 7 February 2019

Guest Editor: Sutasn Thipprakmas

A high-energy mill was designed and built with the purpose of processing magnesium (Mg) powders. The main characteristics of the mill are grinding capacity of 1 kg and demolition elements of 10 kg; it has a distributed form to the interior ten blades of similar geometry, six of which are of the same size and four of them were increased in length in order to avoid the accumulation of the ground material. It has a jacket with a diameter of 240 mm as a cooling system to prevent high temperatures during grinding and possible chemical reactions; likewise, type 304 stainless steel was used for its construction. 10 mills were made during a period of 4, 6, and 8 hours, in order to obtain microparticles; with these particles, an analysis of X-ray spectroscopy was made to verify their physical and chemical characteristics. The outcome shows powder particles with dimensions of 0.1-4 mm, which will be used to the storage and handling hydrogen in the solid state (MgH_2).

1. Introduction

Renewable energy sources are the third largest contributor to global electricity production in 2015 [1]. Renewable energy sources, like solar, wind, biofuels, etc., are needed to mitigate current environmental problems.

Hydrogen is proposed as alternative energy carrier [2]. Hydrogen is the most abundant element in the universe [3]. However, a major problem is the storage of hydrogen, which has to be done safely and with high density. Hydrogen storage in metals has the potential to satisfy these conditions; many metals absorb it [4, 5]. Therefore, world is moving toward the use of metal hydrides, which can "store" per unit cell to two or three times as much hydrogen atoms than the metal itself [6–9]. Metal hydrides are formed by reaction of hydrogen with metals. Deposit metal hydrides and metal compounds containing essentially transition metals and rare earths, with lattices forming interstices which under certain conditions can absorb hydrogen atoms [10]. MgH_2 is studied as a potential hydrogen storage material.

Metal hydrides such as MgH_2 or some complexes as $NaAlH_4$ and $LiAlH_4$ are attractive for this use, store 7.6, 7.3, and 10.1% by weight and hydrogen, respectively, have a low overall weight [11, 12]. Hydrides of pure metals and alloys are an efficient and safe with good hydrogen storage capacity per unit mass storage medium, but generally have slow desorption kinetics and rupture temperatures near 300°C

equilibrium with little stability before repeated cycles of absorption and desorption [13, 14].

In recent studies, the importance of particle size effects on the hydrogen sorption kinetics in Mg and MgH_2 is shown. In that research, the preparation of MgH_2 nanoparticles supported on high surface area carbon aerogels with pore sizes varying from 6 to 20 nm is reported [5]. The metal storage capacity is determined by curves PCT (Pressure, Concentration, and Temperature) [6, 12, 15].

High-energy ball mills equipment is becoming a standard for particle size reduction. This is due to the increasing demand for fine (<1 μm) product particle size and shorter processing cycles [16]. Ball mill is one of the most predominantly used methods for the purpose of mixing and grinding of raw materials [17, 18].

The ball mill process is very complicated process governed by many parameters, such as ball size, ball shape, ball filing, slurry loading (with respect to ball amount), powder loading with respect to the amount of total slurry (slurry viscosity), and rotation speed. A high industrial interest in optimizing such ball mill parameters from the viewpoint of the comminution of ores exists [17].

A recent study reports an optimal ball size for efficient milling with a rotation speed, based on a laboratory-scale wet ball mill. In addition, the effect of powder loading on the particle size reduction has been investigated at given conditions of ball size rotation speed [19]. In ceramic laboratories, ball mill is often carried out to mainly achieve a mixed state powders with initial average particle (d_{50}) of 1-20 μm. In other laboratories, zirconia balls with nominal diameter of approximately 1-10 mm are frequently employed [19]. There have been different studies on the influences of parameters associated with grinding balls such as ball size distribution and ball shape on the particle comminution [20–22].

There are different types of ball mills for obtaining powder, stand out horizontal ball mill (low-energy) and the high efficiency (high-energy) ball mill. The horizontal ball mill was the first equipment used to obtain metastable systems and in the dissolution of metals that exhibit immiscibility. This mill is mounted on rotating rollers by means of which the speed of rotation is controlled, using steel balls, which during the rotation drag the powder cause shock between the particles, deforming and fracturing them, being the basic principle of the alloy mechanics. The equipment is considered low energy and requires extensive grinding times to optimize the same; this type of mill is commonly used in the industry to obtain particles of different materials; these are used in different industries such as cosmetics, mining, metal mechanics, molding of pieces, among others. The mills of high efficiency of grinding work under the principle of the decrease of dead zones; all the materials and the walls of the chamber of the mill are under collision with the balls. This high-energy mill is capable of operation under atmosphere controlled conditions, vacuum, or inert gas, including loading and unloading of powders. High-energy mills are designed primarily for crushing and for laboratory-scale operations [23].

The main difference between mills is the field of application, since the high-energy mill has a scientific application, because advanced materials and small particle sizes (nanometers) are used.

In this study we present the design of a new high-energy mill for the processing of magnesium powders with research objectives; the powder will be used to obtain magnesium hydride (MgH2) and store hydrogen in solid state, with the following objectives:

(i) Obtain magnesium powder, for storage of hydrogen in solid state (hydride), increasing the efficiency of the process through optimum temperature.
(ii) Control the temperature of the mill chamber through a cooling jacket, considering that what is planned obtained primarily pure nanoparticles of magnesium, which will facilitate the storage of hydrogen in the gas phase.

This paper is organized as follows: Section 2 defines the design process of the high-energy mill, as well as the modelling. The manufacturing process is developed in this section. Section 3 defines the process of experimental testing; milling of magnesium is described in detail in this section. In Section 4 the results of the X-ray spectroscopy analysis are shown, where the physical and chemical characteristics of the magnesium particles are verified. Finally, Section 5 presents conclusions and possible future work.

2. Methodology

2.1. Analytical Design and Modelling. For the design of the mill, it was necessary to take certain considerations, which were established based on literature of powder processing, such as the mill capacity (1 kg) and working time (12 hours) in order to have a production of 0.0833 kg/h.

For processing powders with high-energy milling, the use of balls for grinding is indispensable; in the literature it was found that there is a ratio of 10:1; therefore, if the milling capacity is 1 kg, 10 kg balls are needed based on the most conservative parameter. Commonly it used from 30% to 40% of the total mill volume for containing the product to be ground and the grinding elements (steel balls).

The selection of the apparent volume (VA) occupied by the grinding elements arises two litters for optimum performance.

$$V_A = \frac{M_B}{0.7 * \rho_{Steel}} \tag{1}$$

According to the results of previous investigations the total volume (VT) required to contain the grinding elements and the material for grinding is raised in a ratio of 3 to 1 or 3.5 to 1; to accomplish with this requirement the total volume (VT) will be of 6462.25 cm^3.

It is necessary to consider that the machine will be used to grind a mineral, so it is necessary to determine the material of grind (17.287 kW/hr); in this case, the material is magnesium (Mg) and mill production to determine engine power.

$$\begin{aligned} \text{Pe} &= \text{Wi} * \text{Mill production} = \text{Engine power} \\ \text{Pe} &= 17.287\,\text{kW/h} * 0.0833\,\text{kg/h} = 1.44\,\text{kW} \end{aligned} \tag{2}$$

Considering a safety factor of 1.5, the engine power is 2.88 hp.

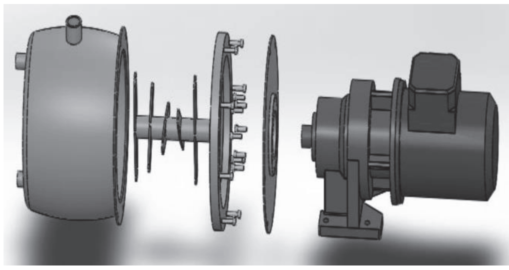

(a)

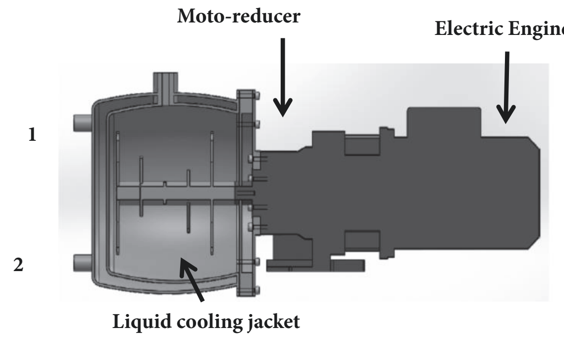

(b)

Figure 1: (a) The main components of the high-energy mill where one indicates the output of the coolant and two input. (b) High-energy mill exploded.

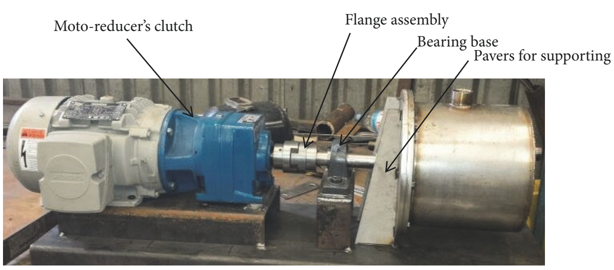

(a)

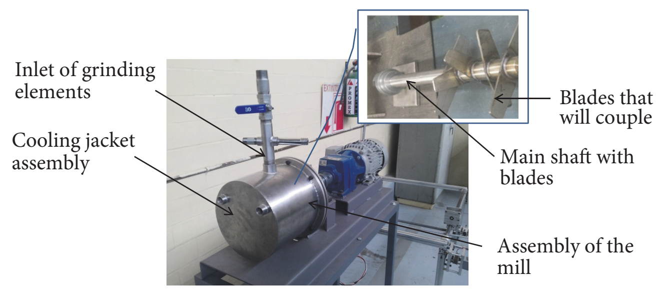

(b)

Figure 2: (a) High-energy mill assembly. (b) Final assembly.

The grinding blades are the transmitter of engine power to the grinding elements. It consisted of a total of ten blades similar geometry, six of the same size and the remaining extend below to avoid agglomeration of the mill base.

The shaft diameter required to transmit the engine power was calculated taking into consideration that the work done is twisted. It should take into account the fact that the engine power is 2.23 kW and the angular speed (ω) at the output of the motor-reducer is 73.32 rad/second. In addition, a yield strength type 304 of stainless steel is 310 MPa with a safety factor of 4. Using the following equation shaft diameter was determined:

$$\tau = \frac{16T}{\pi d^3} < \tau_{adm} \quad (3)$$

To support the impeller efforts, it must be at least 15.88 mm. To design and ensure an ideal coupling with the output of the engine, a shaft of 30 mm was the best for the purpose. Once the analytical development was completed, the development was continued to design through Solidworks® software.

In Figure 1, this modelling describes the components of the mill. (a) The main components of the high-energy mill where one indicates the output of the coolant and two inputs and (b) high-energy mill exploded. This describes the entry and exit of coolant 1 and coolant 2, respectively.

2.2. Construction. The first component built was the tank where magnesium will be ground, having an inlet and an outlet for the coolant; the cooling system will aim to fracture the material and to avoid damage due to the high temperature of the mill. Another important point is to keep the temperature constant during the grinding process, in order to avoid any possible chemical reaction.

Figure 2 shows the assembly of the cooling jacket; it is the most delicate part, because there are two cylinders of different diameters, which are welded in high temperature for the 304 stainless steel for a properly welding; it is important to be sure that it has no leakage and mention that the process of milling particles of magnesium requires a vacuum environment and/or inert, to prevent chemical reaction with oxygen.

The cutting process was performed with laser; likewise, the flange assembly is coupled to the tank; the windmill and the base bearing flange were welded at a high temperature. Coupling the moto-reducer with the axis of the mill shown in Figure 2 must be perfectly leveled to avoid problems of fatigue and premature wear on the main shaft.

The magnesium that was used in the grinding tests has the following thermophysical properties (see Table 1). It was also necessary to carry out a certificate of analysis of the chemical composition of magnesium (see Table 2). The experimental methodology of milling is described below.

The magnesium ingots used in this study are not 100% pure, due to the following considerations:

Table 1: Thermophysical properties of magnesium.

Property	**Value**
Atomic number	12
Valence	2
Oxidation state	+2
Electronegativity	1.2
Covalent radius (Å)	1.30
Ionic radius (Å)	0.65
Atomic radius (Å)	1.60
Electron configuration	[Ne]3s2
First ionization potential (eV)	7.65
Atomic weight (g/mol)	24.305
Density (g/ml)	1.74
Boiling point (°C)	1107
Melting point (°C)	650

Table 2: Certificate of chemical analysis.

Element	Contend
Mg	99.95 %
Ca	0.0020%
Na	-----
Si	0.0090%
Fe	0.0020%
Mn	0.0170%
Ni	0.00030%
Zn	--------
Cu	0.00170%
Al	0.0180%

(i) The technique used in this work is not entirely clean because the plastic deformation between iron balls and magnesium generates impurities, so for this work, the use of magnesium at 99.99 was not considered.

(ii) The importance of this work lies in demonstrating a method that allows grinding magnesium with certain dimensions shown in the images in X-ray spectrum.

(iii) It is considered that the cost of pure magnesium is excessive for this study since the main objective of the work is to grind magnesium with certain dimensions; in addition, it is judged that the difference in the modulus of elasticity between pure magnesium and magnesium allied exceeds 5% for this case study.

(iv) Another justification for the use of magnesium alloy in the amounts to be mill, since the main use of this equipment is to grind large quantities to transport hydrogen.

3. Experimental Test

The system for obtaining magnesium powders is described in Figure 3; it operates with a three-phase electric motor (A) that is coupled to a geared motor (B), which reduces rotation speed from 3600 RPM to 435 RPM in order to increase the torque. The moto-reducer shaft is coupled via a clutch to the shaft of the mill; the speed of the steel balls increases due to the thrust receiving the blades (C), which causes the magnesium have been ground by the shock effect mechanic.

Due to heat generated from collisions between crushing elements and magnesium, a cooling system is implemented; the ball mill has a cooling jacket (C) where it circulates the coolant (glycol) through a hydraulic pump (D); the liquid refrigerant passes through a heat exchanger (F); in order to lower the temperature, the coolant is in a (E) container. The system also has a vacuum pump (G), in order to remove all the air inside the mill. Once reached the maximum vacuum pressure valves V-3 and V-3 are closed. Valves V-2, V-4, and V-5 open and allow the inlet of inert gas “Argon”. Argon is used to maintain stable grinding.

Experimental tests were performed to magnesium milling; the main objective is to obtain nanoparticles of pure Mg. The experimental tests were made under the next conditions: magnesium 1 kg, stainless steel balls 10 kg, temperature 28°C, and vacuum grinding.

Magnesium ingots of 300 grams each were used; these were cut into pieces of 100 grams; it is essential not to saturate large bullion to avoid problems in grinding. Magnesium samples do not need any previous preparation, are at room temperature and for the milling test 10 pieces of 100 grams that is 1 kg, and were used. The size of the demolition elements (balls) was 5 mm. 10 kg of grinding balls was used. The experimental tests were made in a period of time of 4, 6, and 8 hours of milling. The grinding time was established based on the working time established in the design.

The samples obtained were analyzed by scanning electron microscopy in order to determine shape of grain, grain size, uniformity of grain and contamination in the samples. Test scanning electron microscopy was performed in “Centro de Nanociencias y Micro y Nanotecnologías del IPN”.

Scanning electron microscopy (SEM) is the most suitable method used to the study the surface morphology, since the image provided by the SEM is generated by the interaction of an electron beam that sweeps an area on the sample surface, while in light microscopy it is used photons in the visible spectrum. The equipment has a device that generates an electron beam to illuminate the sample and with different detectors is then collected to create an image of the surface that provides information related to forms, textures, and chemical composition. The maximum voltage to excite the electrons is 30 KV. The microscope used in this study is a Quanta 3D FEG (FEI brand). This device includes three secondary electron detectors (SE) optimized for use in high vacuum (HV), low vacuum (LV), and environmental mode (ESEM), as well as a backscattered electron detector (BSE) of solid state.

4. Results

The high-energy mill was designed with a cooling system based on a heat exchanger of cross-flow, to keep it at a constant operating temperature and thereby avoid fatigue of materials due to a high temperature; this design has a system

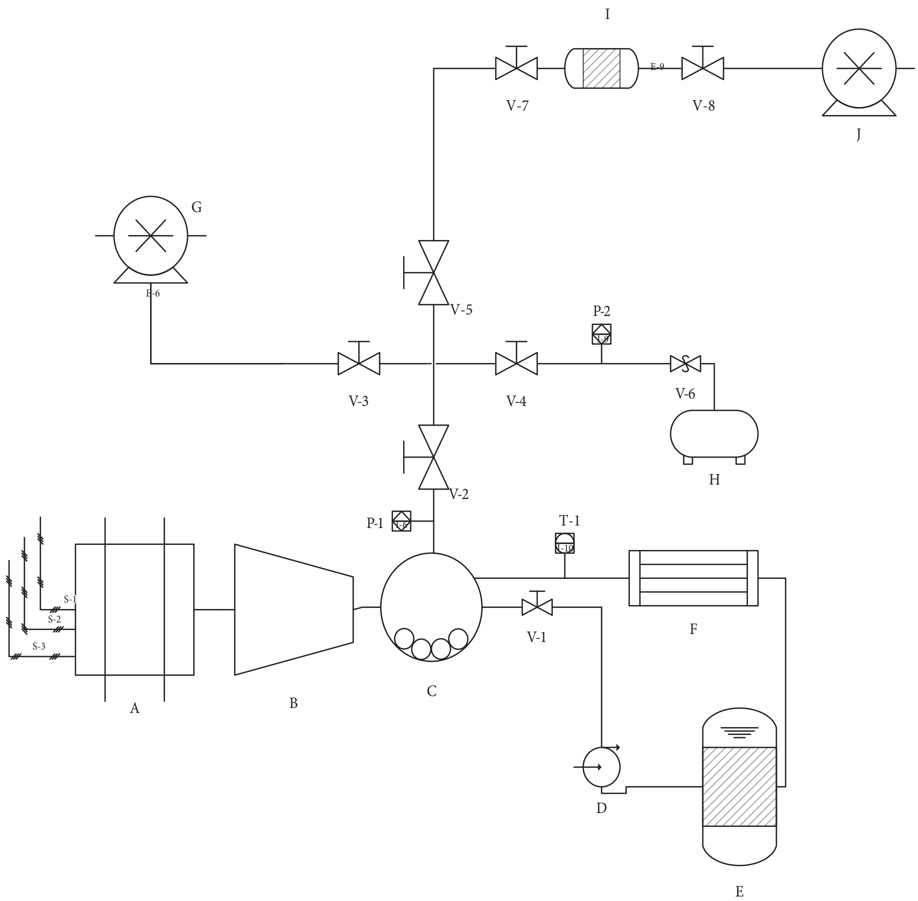

Figure 3: Pneumatic circuit of the high-energy mill.

covering the chamber mill and a compound in which coolant is introduced mainly glycol. To ensure the flow of liquid, the inlet is disposed at one end of the cooling jacket, forcing the fluid to travel the cooling jacket; the outlet is on the opposite side thereof and thus the liquid and it gets stuck and does not allow the system to cool the inside of the mill.

In the camera, the magnesium and the grinding elements were at a constant temperature to avoid fatigue and they were not conducive to a chemical reaction. Because the temperature was kept under control using a cooling jacket, which cover the chamber where the grinding elements work, this cooling jacket works under the principle of operation of a heat exchanger of cross-flow.

The grinding chamber reaches a certain temperature due to the clash between the crushing elements and pieces of magnesium, to have a thermal equilibrium in the grinding and not to promote a chemical reaction; this is wrapped in a cooling jacket, achieving thermal equilibrium.

Another important consideration was that processing magnesium powder must be performed in an inert atmosphere. This atmosphere is created through a pneumatic system, which is connected to the main entrance of the grinding chamber, the same magnesium inlet; once the magnesium is introduced into the mill chamber, vacuum is created through a vacuum pump; once there is no air in the chamber, a controlled amount of Argon is injected to have a completely inert atmosphere to avoid any possible chemical reaction of magnesium. The pneumatic system is also used for the extraction and storage of the product once sprayed.

Figure 4(a) shows that the particles are not uniform with a grinding time of 4 hours; they are of different sizes (particle sizes between 0.1 and 5 mm); the image was taken with an excitation magnetic field of 5.0 KV; the shape of the particles are elongated; the cut is seen very noticeable; this is due to the clash between the ingots; detachment is abundant in burr grinding.

Figure 4(b) shows where a specific image analysis was performed (in the marked box) to determine the percentages of elements in that area

The graphs of X-ray spectrum show that the most abundant element is magnesium with 86.6% by weight. Carbon also has a 10.85% weight but with a 12.94% error in addition to other elements such as oxygen, copper, and zinc with high error rates, which include magnesium ingots used in the milling which are not 100% pure.

Figure 5 shows that the particles are of different sizes (particle sizes between 0.1 and 4 mm), this with a grinding time of 6 hours; the shapes of the magnesium particles are of amorphous type because there is no uniformity of appearance. In Figures 5(b) and 5(d), a slightly more detailed

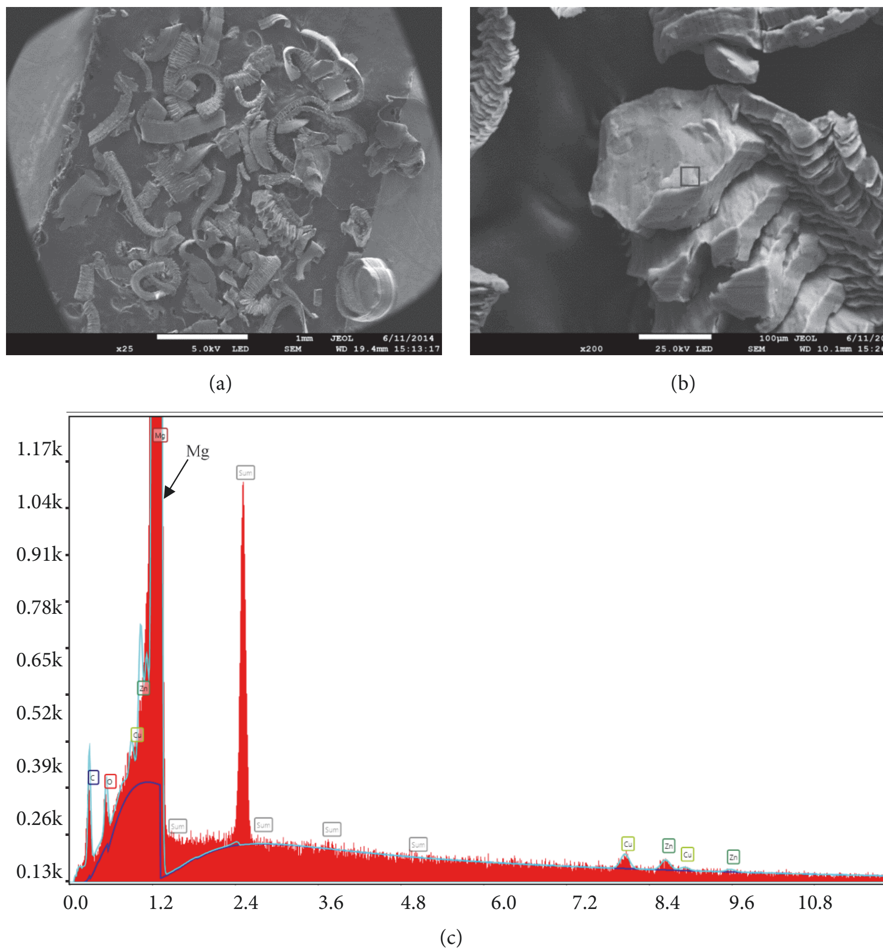

Figure 4: (a) SEM 1A (x 25, 5.0 KV), (b) SEM 1A specific image 1(x200 and 25.0 KV), and (c) results of X-ray spectra.

study shows different features of LED and BED, respectively; in them a trace of elongated shape is observed; this is a contamination of the sample made due to factors such as ingots pollution, pollution of the windmill blades, and release of material from the walls of the mill.

The analysis in Figure 5 shows a substantial percentage of magnesium but there is still contamination by carbon and oxygen. Analysis of X-ray spectrum of Figures 5(b) and 5(d) shows that it is contaminated with other elements such as iron and aluminum. In Figures 6(a), 6(b), and 6(c) with a grinding time of 8 hours, the amount of magnesium is plentiful; even the grain size is not right (particle sizes between 0.1 and 4 mm), but with increasing milling time the uniformity of the particles is noted.

5. Discussion

Breaking metallic materials takes a risk due to the nature of them; they react exothermically if they are suddenly oxidized. Therefore, in this work, the manipulation of them during the high-energy milling process was considered very careful for the own ball mill. The challenge in the development of hydrides is that highly reactive materials are used, as well as pressures and elevated working temperatures; because of that, it was necessary increasing the design requirements of the mill. Performing the milling of magnesium, by means of mechanical manufacture using a high-energy ball mill of its own design, allowed the elaboration of metal particles.

There are different scientific studies that verify the veracity of the high-energy mill.

Osorio et al. found that the statistical models for determining the mechanical efficiency of the mill-cyclone and mill-mill circuits show correlations of 85% and 83%, respectively, and also established that the rotation speed of the mill has no statistical significance and that the most influential parameter for mechanical efficiency is the loading of grinding bodies, which leads to think of a reduction of operational costs to be able to work with low speed values [24]. Graves mentions that an optimum combination of media material properties is very important for efficient operation of the high-energy mill and that some additional media parameters, such as media sphericity and size distribution, will have significant impact on the mill performance [16]. In ceramic laboratories, ball mill is often carried out to mainly achieve a thoroughly mixed state of starting powders with initial average particle (d_{50}) of 1-20 μm. In other laboratories,

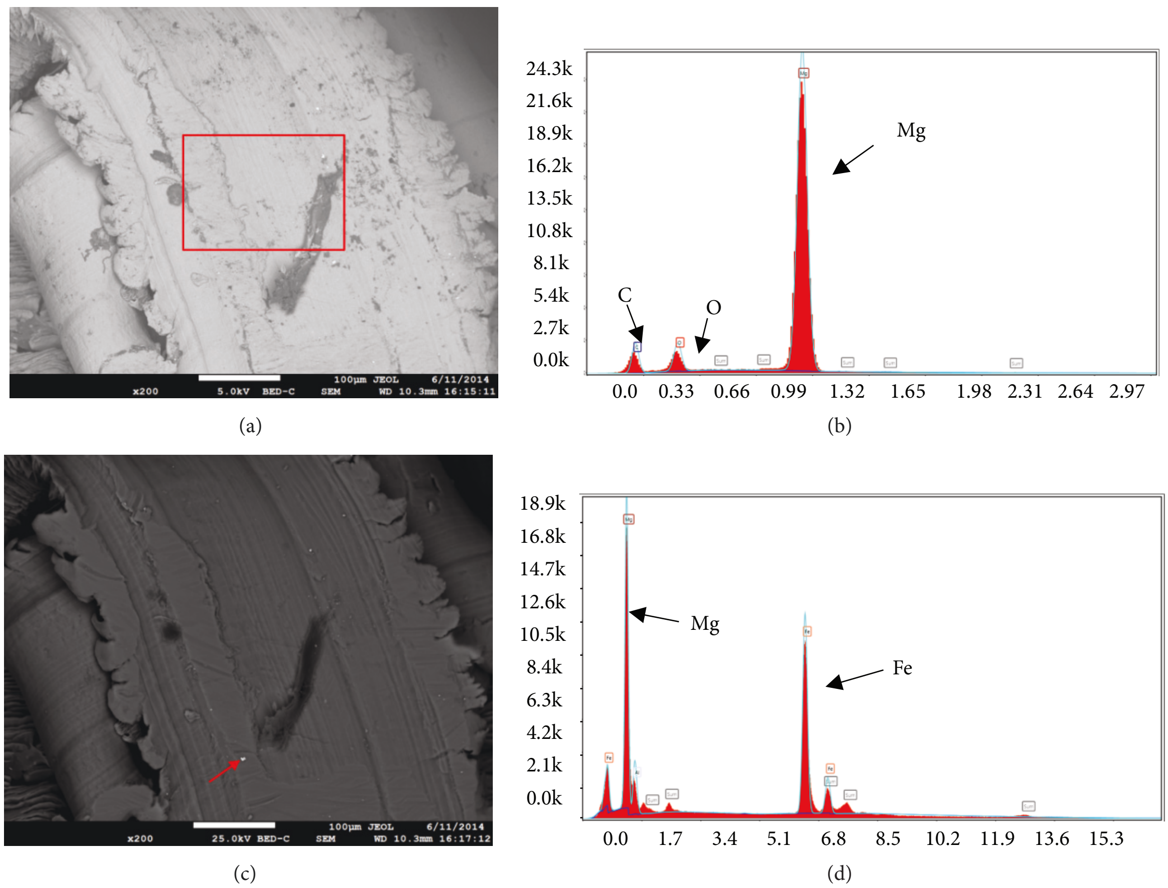

Figure 5: (a) SEM 2A specific image 1, x 200 and 5.0 KV. (b) X-ray spectra. (c) SEM 2A specific image 2, x200, and 5.0 KV. (d) X-ray spectra.

zirconia balls with nominal diameter of approximately 1-10 mm are frequently employed [19].

It is clear that the particle size depends on a large extent on the size of the grinding balls, as mentioned in the related articles. The main difference between this study and the others is the influence of the grinding temperature because a cooling jacket was designed, which aims to control the grinding process under a constant temperature.

The mill reaches a level of grinding between fine and ultra-fine as in commercial equipment (particle sizes between 0.1 and 4 mm), without the restrictions of operation or design presented by them. In addition, the parameters of load of the mill are those that contribute to an effective fragmentation of the equipment of milling (grinding balls 5 mm of diameter), without compromising the quality of the material concluded working time.

The results in this study of the design of the mill for processing magnesium were satisfactory to obtain good functionality, optimal work in grinding, stable temperatures, minimum mechanical vibration, and a correct general operation of the mill, however; the objective of obtaining nanoparticles was not reached; we consider that we do not use the appropriate grinding balls; other similar studies frequently use zirconia balls between 1 and 10 mm of nominal diameter, to obtain particles of 1-20 μm. [19]. As for the cooling system that was designed, no temperatures higher than 100°C were recorded (in the cooling system); it would be convenient in future works to incorporate temperature sensors in different points of the cooling system even inside the chamber of grinding.

According to the experience of the authors during the experimental tests of milling of magnesium, it is established that the optimization required to the mill can be carried out under three areas:

(i) Mechanical, where they try to make numerical models through MEF that allow knowing the fatigue of materials that comprise the milling system.

(ii) Automation of the mill: it is necessary to implement a heuristics method that allows the modulation of the temperature and monitor the amount of explosive gases in the grinding chamber, in order to control the hydration process with high safety standards.

(iii) Inspection of the sample: it is necessary to apply a visual system to monitor the size of the particle in order to control the grinding times.

To store hydrogen in the solid state, particle sizes of (6-20 nm) are reported [5]. In a future work, experimental tests with grinding ball diameters of less than 5 mm will be carried out, dry reactive grinding tests (MRS) will be carried out, and the

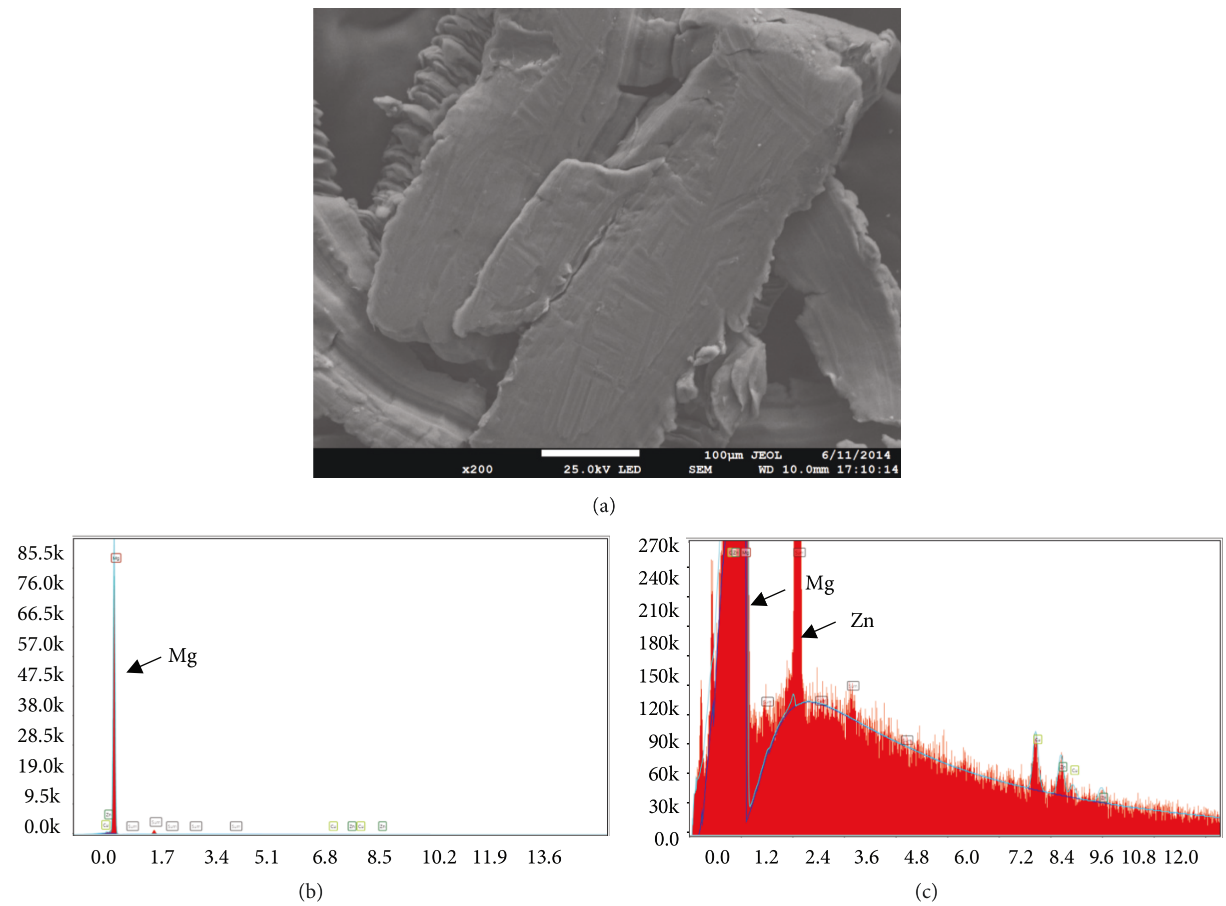

Figure 6: (a) SEM 3A, x200, and 25.0 KV, LED. (b) X-ray spectra. (c) X-ray spectra.

formation of magnesium hydrides by diffraction (DXR) will be demonstrated, as well as the possible pollutants produced by mechanical energy.

6. Conclusion

A high-energy mill was designed, built, and operated to process magnesium powder. The mill has a milling capacity of 1 kg and 10 kg crushing elements (diameter 5 mm); it consists of a total of ten blades similar geometry, six of which are the same size and four extend below to avoid agglomeration of the mill base. It has a cooling jacket to avoid high temperatures and thus grinding favors the milling process. A tire air extraction system and injection of argon are also designed and implemented because the magnesium powder processing must be vacuum or in an inert atmosphere.

A tire air extraction system and injection of argon are also designed and implemented because the magnesium powder processing must be vacuum or in an inert atmosphere.

The samples obtained were analyzed by scanning electron microscopy in order to determine

(i) the grain shape;

(ii) the grain size;

(iii) uniformity of grain in the sample;

(iv) sample contamination.

In sample 1A (4 hours of grinding), it is possible to note that the particles are not uniform and is of different sizes; the image was taken with an excitation magnetic field of 5.0 KV; the shape of the particles is elongated and is seen very well known; this is due the clash between the ingots; detachment is abundant in burr grinding. The particle sizes are between 0.1 and 5 mm.

In sample 2A (6 hours of grinding), the particles are of different sizes (particle sizes between 0.1 and 4 mm); the shape of the magnesium particles is amorphous because there is no uniformity of appearance. Sample contamination is observed due to factors such as pollution ingots, pollution of the windmill blades, and detachment of material from the walls of the mill. The analysis of X-ray spectrum shows that it is contaminated with iron and other elements such as aluminum.

Sample 3A (8 hours of grinding) shows that magnesium is abundant (particle sizes between 0.1 and 4 mm); even the grain size is not right, but with increasing milling time the uniformity of the particles is observed; it is important to mention that, in order to store hydrogen, is necessary that the magnesium particles have a particle size of nanometers.

The efficiency of the high-energy mill is a multifactorial process that depends on different factors. It is commonly accepted that high-energy mill processes are based on the assumption that high the mill is operated under conditions of full media fluidization; i.e., fluidization conditions are determined by a combination of media properties (density, size, and mill volume), product properties (density, size, and mill volume), product properties (density, % solids, and viscosity at processing conditions), and mill operating conditions (product feed rates and shaker speed) [17].

Particle size depends on the size of the demolition elements. If increase in the balls grinding the result will increase dead zones, which would imply a deficiency in the grinding process, the same happens with a high number of blades.

With the results obtained in this study it is possible to obtain a mathematical model of the grinding process; the most important variables to consider in this model would be size of demolition elements, speed of the engine rotation, temperature of the grinding process, and time of the process.

Researchers community requires high-precision machines and processes; as a future objective, it will be considered the methodology reported by [25] for the conceptual redesign and FEM validation, for this customized experimental equipment used in magnesium grinding; it will be possible to estimate the total machine flexibility for other process conditions in a convenient and easy manner. Also, the application of these methodologies will allow finding the tolerances and the accuracy of all components that have the milling system (chamber, blades, and balls) with the purpose to establish the durability of the high-energy ball mill.

Data Availability

The design, modelling, mathematical calculations, manufacturing process, scanning electron microscopy studies, and X-ray spectrum data used to support the findings of this study are included within the article.

Conflicts of Interest

The authors J.C. Paredes Rojas, L.E. Álvarez Ramírez, G. Urriolagoitia Sosa, C.R. Torres San Miguel, B. Romero Ángeles, J. A. Leal Naranjo, and G. M. Urriolagoitia Calderón declare that there are no conflicts of interest regarding the publication of this paper.

Authors' Contributions

All authors have approved the manuscript and agree with its submission to the Journal "Mathematical Problems in Engineering".

Acknowledgments

Thanks are due to the CONACYT-Mexico Scholarship granted to Juan Carlos Paredes, to the research team of the Automotive Systems Engineering Laboratory of the ESIME UC-IPN-Mexico, and to Sección de Estudios de Posgrado e Investigación of ESIME ZAC. The authors gratefully acknowledge the financial support from the Mexican Government by Consejo Nacional de Ciencia y Tecnología, to the Instituto Politécnico Nacional. The authors also acknowledge partial support by Projects 20181141 and 1931, as well as EDI grant, all provided by SIP/IPN.

References

[1] IEA, "International energy agency, statistics renewables information," 2017, http://www.iea.org/topics/renewables/.

[2] G. W. Crabtree, M. S. Dresselhaus, and M. V. Buchanan, "The hydrogen economy," *Physics Today*, vol. 57, no. 12, pp. 39–44, 2004.

[3] D. A. J. Rand and R. M. Dell, *Hydrogen Energy: Changes and Prospects*, RSC Energy Series, RSC Publishing, 2008.

[4] M. Hirscher, *Handbook of Hydrogen Storage: New Materials for futurEnergy Storage*, Wiley-VCH, Weinheim, Germany, 2010.

[5] Y. S. Au, M. K. Obbink, S. Srinivasan, P. C. M. M. Magusin, K. P. De Jong, and P. E. De Jongh, "The size dependence of hydrogen mobility and sorption kinetics for carbon-supported MgH2 particles," *Advanced Functional Materials*, vol. 24, no. 23, pp. 3604–3611, 2014.

[6] I. A. Vertiz, *Análisis experimental de almacenamiento de hidrógeno en estructuras sólidas, Tesis de Doctorado en Diseño*, Instituto Politécnico Nacional, México, 2012.

[7] J. R. Mihelcic and J. B. Zimmerman, *Ingeniería Ambiental*, Editorial Alfaomega, México, 2011.

[8] J. P. Blackledge, *Metal Hydrides*, Academic Press, New York, NY, USA, 1968.

[9] F. A. Cotton and G. Wilkinson, *Advanced Inorganic Chemistry: a comprehensive text*, John Wiley & Sons, EE.UU, 1980.

[10] E. I. Zoulias and N. Lymberopoulos, *Hydrogen-based Autonomous Power Systems*, Springer -Verlag 1, London, UK, 2008.

[11] L. Schlapbach and A. Züttel, "Hydrogen-storage materials for mobile applications," *Nature*, vol. 414, no. 6861, pp. 353–358, 2001.

[12] F. C. Gennari and F. J. Castro, "Formation, composition and stability of Mg-Co compounds," *Journal of Alloys and Compounds*, vol. 396, no. 1-2, pp. 182–192, 2005.

[13] B. Molinas, A. A. Ghilarducci, M. Melnichuk et al., "Scaled-up production of a promising Mg-based hydride for hydrogen storage," *International Journal of Hydrogen Energy*, vol. 34, no. 10, pp. 4597–4601, 2009.

[14] M. Verga, F. Armanasco, C. Guardamagna et al., "Scaling up effects of Mg hydride in a temperature and pressure-controlled hydrogen storage device," *International Journal of Hydrogen Energy*, vol. 34, no. 10, pp. 4602–4610, 2009.

[15] B. Vigeholm, J. Kjoller, B. Larsen, and A. S. Pedersen, "Formation and decomposition of magnesium hydride," *Journal of the Less-Common Metals*, vol. 89, no. 1, pp. 135–144, 1982.

[16] G. A. Graves and T. Boehm, "Mill media considerations for high energy mills," *Minerals Engineering*, vol. 20, no. 4, pp. 342–347, 2007.

[17] L. G. Austin, R. R. Klimpel, and P. T. Luckie, *The Process Engineering of Size Reduction: Ball Milling*, Society for Mining Metallurgy & Exploration, Englewood, 1984.

[18] T. Tokmakci, A. Ozturk, and J. Park, "Boron and zirconium co-doped TiO_2 powders prepared through mechanical ball milling," *Ceramics International*, vol. 39, no. 5, pp. 5893–5899, 2013.

[19] H. Shin, S. Lee, H. Suk Jung, and J.-B. Kim, "Effect of ball size and powder loading on the milling efficiency of a laboratory-scale wet ball mill," *Ceramics International*, vol. 39, no. 8, pp. 8963–8968, 2013.

[20] T. M. Cook and T. H. Courtney, "The effects of ball size distribution on attritor efficiency," *Metallurgical and Materials Transactions A: Physical Metallurgy and Materials Science*, vol. 26, no. 9, pp. 2389–2397, 1995.

[21] F. M. Katubilwa and M. H. Moys, "Effect of ball size distribution on milling rate," *Minerals Engineering*, vol. 22, no. 15, pp. 1283–1288, 2009.

[22] N. S. Lameck, K. K. Kiangi, and M. H. Moys, "Effects of grinding media shapes on load behaviour and mill power in a dry ball mill," *Minerals Engineering*, vol. 19, no. 13, pp. 1357–1361, 2006.

[23] D. Basset, P. Matteazzi, and F. Miani, "Designing a high energy ball-mill for synthesis of nanophase materials in large quantities," *Materials Science and Engineering: A Structural Materials: Properties, Microstructure and Processing*, vol. 168, no. 2, pp. 149–152, 1993.

[24] A. M. Osorio, J. M. Marín, and G. Restrepo, "Diseño y evaluación energética de dos circuitos de molienda y clasificación para un clinker de cemento a escala piloto," *Información tecnológica*, vol. 24, no. 2, pp. 99–108, 2013.

[25] D. Del Pozo, L. N. López de Lacalle, J. M. López, and A. Hernández, "Prediction of press/die deformation for an accurate manufacturing of drawing dies," *The International Journal of Advanced Manufacturing Technology*, vol. 37, no. 7-8, pp. 649–656, 2008.


Advances in Operations Research
Advances in Decision Sciences
Journal of Applied Mathematics
The Scientific World Journal
Journal of Probability and Statistics
International Journal of Mathematics and Mathematical Sciences
Hindawi
Submit your manuscripts at
www.hindawi.com
Journal of Optimization
International Journal of Engineering Mathematics
International Journal of Analysis
Journal of Complex Analysis
Advances in Numerical Analysis
Mathematical Problems in Engineering
International Journal of Differential Equations
Discrete Dynamics in Nature and Society
International Journal of Stochastic Analysis
Journal of Mathematics
Journal of Function Spaces
Abstract and Applied Analysis
Advances in Mathematical Physics